Journal of Solid State Chemistry 184 (2011) 649–654

Contents lists available at ScienceDirect

Journal of Solid State Chemistry

journal homepage: www.elsevier.com/locate/jssc

Crystallographic and magnetic characterisation of the brownmillerite $Sr_2Co_2O_5$

Eirin Sullivan [a,1], Joke Hadermann [b], Colin Greaves [a,*]

[a] School of Chemistry, University of Birmingham, Birmingham B15 2TT, UK
[b] EMAT, University of Antwerp Groenenborgerlaan 171, B-2020 Antwerp, Belgium

ARTICLE INFO

Article history:
Received 30 September 2010
Received in revised form
22 December 2010
Accepted 17 January 2011
Available online 26 January 2011

Keywords:
$Sr_2Co_2O_5$
Brownmillerite
Oxygen order
Neutron diffraction
Magnetic structure
Electron diffraction

ABSTRACT

$Sr_2Co_2O_5$ with the perovskite-related brownmillerite structure has been synthesised via quenching, with the orthorhombic unit cell parameters $a=5.4639(3)$ Å, $b=15.6486(8)$ Å and $c=5.5667(3)$ Å based on refinement of neutron powder diffraction data collected at 4 K. Electron microscopy revealed L–R–L–R-intralayer ordering of chain orientations, which require a doubling of the unit cell along the *c*-parameter, consistent with the assignment of the space group *Pcmb*. However, on the length scale pertinent to NPD, no long-range order is observed and the disordered space group *Imma* appears more appropriate. The magnetic structure corresponds to G-type order with a moment of 3.00(4) μ_B directed along [1 0 0].

1. Introduction

Brownmillerite materials exhibit a distinctive oxygen-deficient perovskite structure in which the oxygen vacancies are ordered within planes to provide alternating layers of cations in corner linked octahedra and tetrahedra. The layers of tetrahedral cations comprise chains, which are directed along a single direction to provide overall orthorhombic symmetry; the chain direction defines the *a*-axis and the alternating octahedral/tetrahedral layers are perpendicular to the *b*-axis. Each chain displays co-operative rotations of the individual tetrahedra to provide appropriate metal–oxygen bond distances. Subtle differences in symmetry can occur depending on the order that exists relating to the sense of the rotation of the tetrahedra within a given layer, and also that between adjacent layers. Although the tetrahedral chains are fully ordered within a given layer, the chain rotations may order (*Pnma* or *I2mb* symmetry) or disorder (*Imma* symmetry) with respect to adjacent layers. The relationship between chain ordering and symmetry in this structure is interesting and possibly relevant to the properties displayed by this class of materials, e.g. the observation of colossal magnetoresistance in $SrCaMnGaO_5$ [1]. A detailed description of the factors determining the possible schemes for oxygen order, including the existence of intralayer order to give doubling of the unit cell along [0 0 1] can be found elsewhere [2,3,4].

Takeda et al. [5] determined that $Sr_2Co_2O_5$ with brownmillerite-type structure is an antiferromagnet with a Néel temperature of 570 K. Neutron powder diffraction showed this material to exhibit a G-type magnetic structure ($\mu=3.3(5)$ μ_B at 77 K) and the unit cell parameters at 168 °C were reported as $a=5.4761(3)$ Å, $b=15.8016(10)$ Å and $c=5.5819(3)$ Å after transposing for consistency with the space group *Imma*. This material is essentially isostructural with $Sr_2Fe_2O_5$ [6] and Sr_2CoFeO_5 [7]. The orthorhombic unit cell is related to the basic perovskite unit cell dimension, a_p, by $a\approx\sqrt{2}a_p$, $b\approx 4a_p$, $c\approx\sqrt{2}a_p$ and the oxygen-deficient layers of CoO_4 tetrahedra are at $y=0.25$ and 0.75. The brownmillerite-type polymorph of $Sr_2Co_2O_5$ is metastable and only formed by quenching from temperatures above ≈910 °C [8]. On slow cooling, the high temperature cubic perovskite form transforms at ~750 °C to give the thermodynamically stable low temperature configuration [9], which was subsequently shown to comprise an intergrowth of two phases: rhombohedral $Sr_6Co_5O_{15}$ (2H $BaNiO_3$-type) and Co_3O_4 [10]. Upon quenching, the brownmillerite-type phase $Sr_2Co_2O_5$ is stabilised by high spin (HS) Co^{3+} cations in octahedral and tetrahedral coordination; both sites have four unpaired electrons with configurations $t_{2g}^4e_g^2$ and $e^3t_2^3$, respectively [8,11]. *Ab initio* work by Muñoz et al. [12] supported the hypothesis that this material contains Co^{3+} in a high spin state. Density functional theory calculations based upon $Sr_2Co_2O_5$ as a high-spin system [13] confirmed a stable G-type antiferromagnetic structure. The magnetic structure of $Sr_2Co_2O_5$ is shown in Fig. 1, with Sr and O atoms omitted for clarity. It should be noted that Takeda et al. [5] originally described this structure using the *Icmm* space group (the **cba** setting of *Imma*) and

* Corresponding author. Fax: +44 121 414 4442.
E-mail address: c.greaves@bham.ac.uk (C. Greaves).
[1] Nanocenter, University of South Carolina, SC 29208, USA.

0022-4596/$ - see front matter © 2011 Elsevier Inc. All rights reserved.
doi:10.1016/j.jssc.2011.01.026

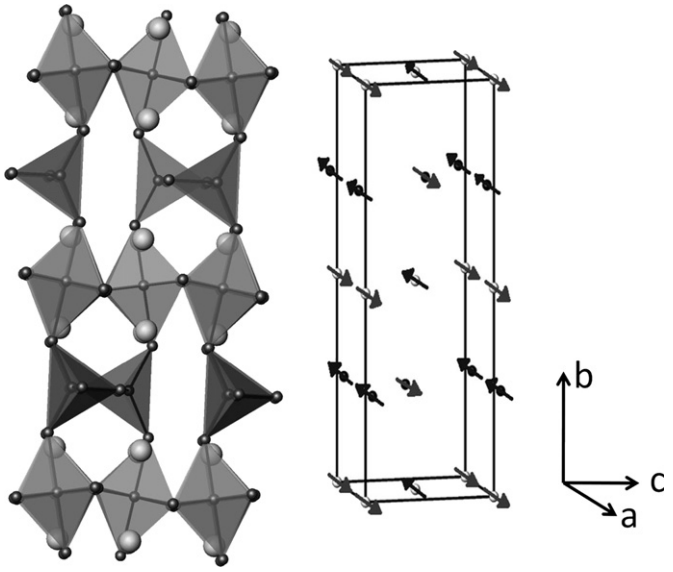

Fig. 1. The crystallographic structure and G-type antiferromagnetic structure of $Sr_2Co_2O_5$ with the Co^{3+} spins directed along the *a*-axis.

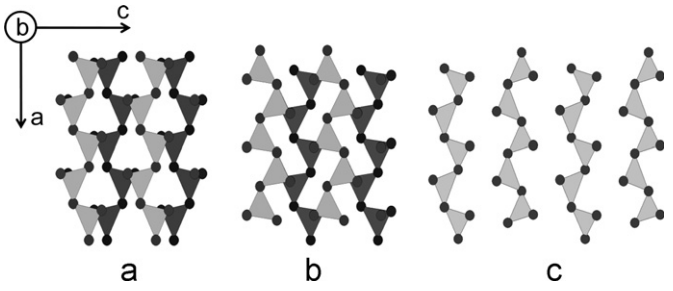

Fig. 2. Tetrahedral chain orientation at $y=0.25$ (light grey) and $y=0.75$ (dark grey): (a) identical interlayer orientation as described by the space group *I2mb*; (b) interlayer alternation as described by the space group *Pnma*; and (c) intralayer L–R–L–R alternation as described by the space group *Pcmb*.

reported that the Co^{3+} spins are directed along the shortest axis (which in *Icmm* is the *c*-axis). For facile comparison with the space groups *I2mb*, *Pnma* and *Pcmb*, the standard setting for this space group, *Imma*, has been used with the spins therefore directed along the *a*-axis. In a more recent structural study, the structure has been represented using the ordered *I2mb* space group [14].

Although the structures of brownmillerites (generic representation $A_2B_2O_5$) are very closely related, small differences in symmetry arise due to the intra- and inter-layer orientational order of the infinite chains of BO_4 tetrahedra. For the tetrahedral chains (and vacancy strings) directed along [1 0 0] and the layers of BO_4 tetrahedra perpendicular to [0 1 0], displacements of O and B atoms occur to provide pseudo-tetrahedral geometry for the B atoms, and these displacements can occur in two equivalent fashions: [1 0 0] and [$\bar{1}$ 0 0]. The resultant tetrahedral chains can be represented as L-chains or R-chains and order between these types of chain provides different structures [15,16].

Three basic structures contain only a single type of chain (L or R) within a given layer. If adjacent BO layers have the same chain orientation (only L- or R-chains throughout the structure) (Fig. 2(a)) the arrangement is consistent with the non-centrosymmetric space group *I2mb*. If layers of L-chains alternate with layers of R-chains, the structure is centrosymmetric, space group *Pnma* (Fig. 2(b)). Finally, a totally disordered arrangement of the two possible layer types provides, on average, a random distribution of L- and R-chains throughout the structure, consistent with space group *Imma*.

A fourth type of chain order has been reported in Sr_2MnGaO_5 [17,18], which contains MnO_2 (octahedral Mn) and GaO (tetrahedral Ga) layers. Electron diffraction and high-resolution electron microscopy revealed alternation of L- and R-chains within a given layer resulting in doubling of the *c*-axis (Fig. 2(c)) to give a supercell with *Pcmb* symmetry: $a \approx \sqrt{2}a_p$, $b \approx 4a_p$, $c \approx 2\sqrt{2}a_p$ [19]. This type of intralayer order was also found in $Sr_2Fe_2O_5$. In this compound several order patterns were subsequently found to exist between the layers themselves. A detailed description of the different types of order observed, together with the effects on diffraction patterns and a general monoclinic model in 3+1-dimensional space can be found in Ref. [20]. Differences in ordering of the tetrahedral chains within the layer have also been observed by Krüger et al. for $Ca_2Fe_2O_5$ [21,22], albeit this time in an incommensurately modulated fashion. Indeed, many brownmillerite-type structures have been shown, upon closer observation, to exhibit commensurately or incommensurately modulated ordering of tetrahedral chains. Abakumov et al. [2] proposed that a possible driving force for the different tetrahedral chain ordering patterns observed in brownmillerites could be the minimisation of free energy due to the interaction between the dipole moments of tetrahedral chains.

Although $Sr_2Co_2O_5$ has previously been reported to crystallise in the disordered space group *Imma*, no significant difference between the models was apparent in structural data, and descriptions using *Imma* and *I2mb* can be found [5,12,14]. However, the distance between the tetrahedral layers (7.9 Å [12]) and the deviation from 180° of the Co–O–Co angle in the tetrahedral layer (angle of 117.4° [12]) are large. According to the relations proposed in [3] between these two parameters and the L–R order, $Sr_2Co_2O_5$ would therefore be expected to show intralayer L–R–L–R order. Given that the calculations previously reported [12] did not explore a structure involving such intralayer order, the aim of this study was therefore to use electron diffraction and neutron powder diffraction to probe in detail the chain ordering in $Sr_2Co_2O_5$ and hence perform a more complete structural and magnetic characterisation of this material.

2. Experimental

A polycrystalline sample of brownmillerite $Sr_2Co_2O_5$ was synthesised by the standard solid-state reaction of stoichiometric quantities of high purity $SrCO_3$ and Co_3O_4. The reagents were ground together and subjected to 2 heat treatments with intermediary grinding, consisting of 12 h at 1150 °C in air. The second heat treatment was followed by immediately quenching from 1150 °C into liquid nitrogen.

Electron diffraction patterns were taken on a Phillips CM20. High-resolution transmission electron microscopy images were taken on a JEOL 4000EX. The samples for the TEM investigations were prepared by crushing the powder in an agate mortar, dispersing the powder in ethanol and evaporating drops of this dispersion on a copper grid covered with a holey carbon layer.

Neutron powder diffraction was carried out at the Institut Laue-Langevin, Grenoble using the high-resolution, two-axis powder diffractometer D2B (Ge monochromator, $\lambda=1.59432$ Å) operating in high intensity mode. The sample was contained in an 8 mm vanadium can and data were collected at temperatures of 300, 200, 100 and 4 K. The GSAS suite of programs [23,24] was used to carry out Rietveld structure refinement [25,26] with linear interpolation function background parameters, diffractometer zero point, histogram scale factor, lattice parameters, pseudo-Voigt peak profiles, atomic co-ordinates and isotropic thermal parameters refined.

3. Results and discussion

3.1. Electron microscopy

To explore the possibility of chain ordering more rigorously, the sample was examined by electron diffraction (ED). The ED patterns are shown in Figs. 3–5 and are indexed according to the disordered brownmillerite space group *Imma.* The ED patterns along the [0 1 0] zone axis (Fig. 3) display sharp superstructure reflections corresponding to $(h, 0, l+1/2)$ indicating a doubling of *c.* This shows that there is intralayer L–R–L–R ordering, as expected based upon the relations given in Ref. [3]. The ED patterns of other main zones [1 0 0] and [1 0 1] do not show any special features. High-resolution images of the [0 1 0] zone show this doubling of the *c*-parameter as a contrast variation with a periodicity of approximately 11 Å along [0 0 1] (Fig. 6). To determine the character of the interlayer order (these L–R–L–R layers can be stacked in different ways), one has to focus on the ED pattern of the [1 0 2] zone (Fig. 4), as explained in detail in Ref. [19]. In $Sr_2Co_2O_5$ the most frequently observed pattern for this [1 0 2] zone is the one shown in Fig. 4 (left side). Comparing this pattern with the schemes and tables in Ref. [19] leads to the conclusion that the structure corresponds to a *Pcmb* ordered structure, i.e. the L–R–L–R layers are ordered in a staggered manner along the *b*-axis. However, within the same crystallites areas were also present with [1 0 2] ED patterns as shown in Fig. 4 (right side). The discrete reflections are replaced by continuous streaks. This proves that the interlayer ordering is only short range. The intralayer ordering, on the contrary, prevails also in these areas, since the streaks are still at positions corresponding to a doubled *c*-parameter, and the streaks show disorder along *b* only.

The electron diffraction study also shows extensive twinning in the crystals as previously discussed [15]; an example is presented in Fig. 5, showing a twinned pattern of the [1 0 0] and $[\bar{2}\,1\,\bar{2}]$ patterns. Many other examples of twinning in $Sr_2Co_2O_5$ could be shown, but for this example, both zones are clearly recognisable. Note also that the $[\bar{2}\,1\,\bar{2}]$ ED pattern clearly shows the doubling of the periodicity along the *c*-parameter through the presence of reflections $0,k,l+1/2$.

3.2. Structure refinement based on NPD data

Neutron powder diffraction data were collected at 4 K in order to examine whether the *Pcmb* symmetry was still reflected on the longer length scale applicable to the neutron wavelength, and to provide more complete structural and magnetic characterisation. In order to account for the magnetic component of the NPD data, the refinement was carried out in terms of 2 phases, one purely nuclear and the other purely magnetic.

As indicated by electron diffraction, a structural model for $Sr_2Co_2O_5$ based on Sr_2MnGaO_5 was adopted for the nuclear component of the refinement, with doubling of the *c*-parameter due to the L–R–L–R-ordering of chain orientations within each tetrahedral layer. The magnetic model was based upon G-type antiferromagnetic order with the Co^{3+} moments directed along the *a*-axis as proposed by Takeda et al. [5]. *Pcmb* was used as a fully ordered model for the magnetic unit cell (4 Co positions: octahedral Co(1) and Co(3), tetrahedral Co(2) and Co(4)) with the lattice parameters of both the nuclear and the magnetic phases constrained to be equal. The temperature factors of the same atomic species were constrained to remain equal to assist with the stability of the refinement.

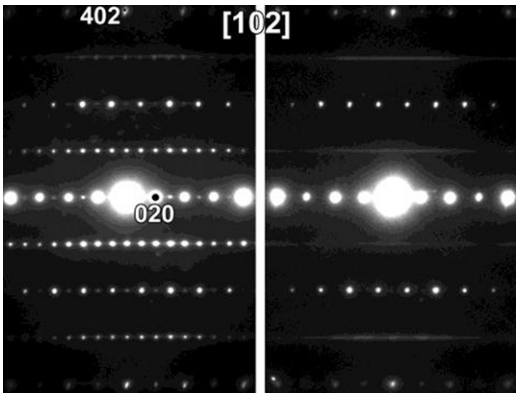

Fig. 4. Electron diffraction patterns of the [1 0 2] zone of $Sr_2Co_2O_5$. The left pattern shows an area with intralayer order-interlayer order corresponding to *Pcmb*, the right pattern shows intralayer order-interlayer disorder. (The indexes refer to the *Imma* cell.)

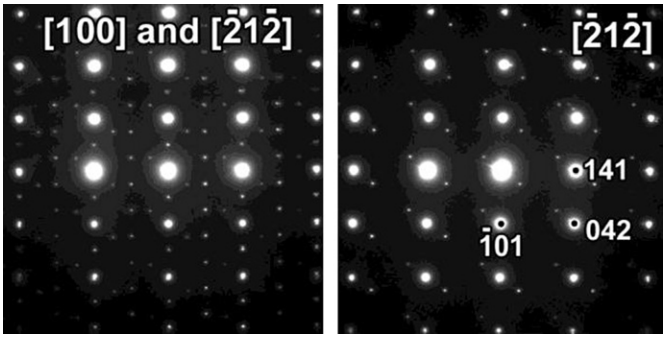

Fig. 5. *Left*: electron diffraction pattern of a typical twinned area, showing overlap of [1 0 0] and $[\bar{2}\,1\,\bar{2}]$; *Right*: the $[\bar{2}\,1\,\bar{2}]$ component in this twin obtained by careful selection of a [100]-free area by aperture. (The indexes refer to the *Imma* cell.)

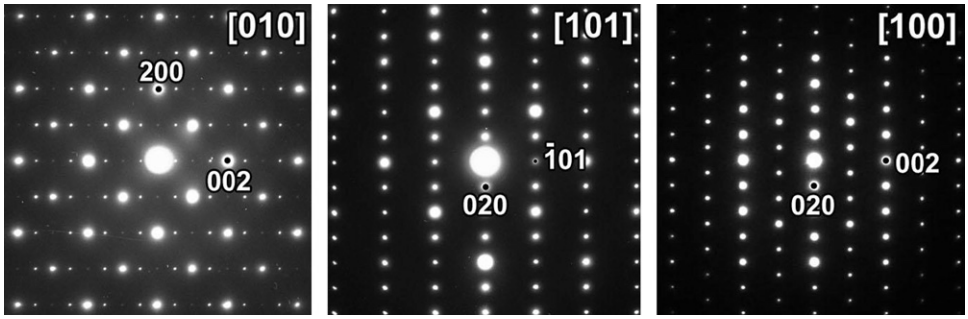

Fig. 3. Electron diffraction patterns corresponding to the cubic subcell ⟨1 0 0⟩ zones of $Sr_2Co_2O_5$. (The indexes refer to the *Imma* cell.)

The nuclear and magnetic refinement proceeded satisfactorily in the space group *Pcmb*, consistent with doubling of the *c*-parameter ($a=5.4640(3)$ Å, $b=15.6485(8)$ Å, $c=11.1340(6)$ Å, $\chi^2=5.080$, $R_{wp}=3.76\%$, $R_p=2.76\%$,) and the presence of a superstructure. For the magnetic refinement, a single magnetic moment was assigned for both octahedral and tetrahedral Co, with all moments aligned along the *a*-axis, giving a refined magnetic moment per $Co^{3+}=2.80(4)\,\mu_B$ which is significantly lower than that reported by Takeda et al. [5] ($\mu=3.3(5)\,\mu_B$ at 77 K). Inspection of the bond lengths obtained from this refinement, however, revealed significant discrepancies in the Co–O bond lengths: the Co(3) octahedra were markedly smaller (~9%) than the Co(1) octahedra and in the tetrahedral layers, one of the Co(4)–O bonds was unrealistically short (1.68 Å) whilst another was very long (2.19 Å). Moreover, very careful examination of the NPD observed profile revealed no significant intensities for reflections that would demand a doubling of the *c*-parameter. Although some superstructure reflections may well be too weak to be observed in refinements based upon powder diffraction data for such brownmillerite-type materials, no evidence for symmetry reduction or cell enlargement was found. In the case of $Ca_2Fe_2O_5$, this material has been well-characterised as crystallising in *Pnma* from polycrystalline data [27,28], yet more recently single-crystal samples have been shown to display an incommensurately modulated superstructure [21,22]. After consideration of bond valence sum calculations, it was concluded that in this particular case the observed difference in Co–O bond lengths for $Sr_2Co_2O_5$ could well be an artefact of using a doubled unit cell i.e. an inappropriate space group for the data. This conclusion is reminiscent of the work by Lindberg et al. [29] on $Sr_2Co_{2-x}Al_xO_5$ ($0.3 \le x \le 0.5$) whereby refinement based upon XRD using the tetragonal unit cell $a \approx a_{per}$, $c \approx 2a_{per}$ fitted the data well and was a suitable description of the bulk phase even though crystallites consisting of small domains with brownmillerite-type structure were observed in ED and HRTEM images.

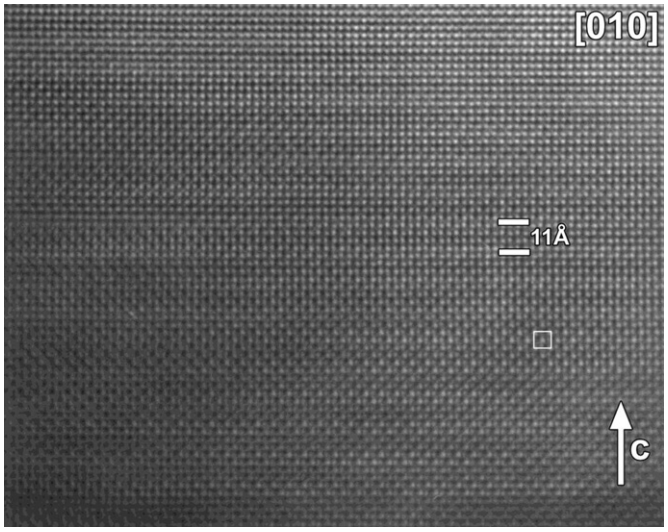

Fig. 6. High-resolution transmission electron microscopy image of $Sr_2Co_2O_5$ viewed along the [0 1 0] axis, illustrating the periodicity of approximately 11 Å.

In order to evaluate whether other possible models of chain ordering might provide a better fit, structure refinements based on the various possible brownmillerite subcells were performed. Structural refinement based upon NPD data in the space group *I2mb* resulted in significantly worse statistics than the *Pcmb* refinement ($\chi^2=9.706$, $R_{wp}=5.22\%$, $R_p=3.98\%$). This is unsurprising that the chain ordering observed *via* electron diffraction consisted solely of intralayer alternation of tetrahedral chain orientation. None of the crystallites studied displayed *I2mb* symmetry (identical tetrahedral chain orientation in all layers) thus it follows that using the fully ordered space group *I2mb* would most likely result in a worse fit for the data in this case.

It should be noted that de la Calle et al. [14] have presented NPD data collected on a polycrystalline sample of $Sr_2Co_2O_5$, which fits the fully ordered *I2mb* structural model very well. The sample studied in this paper was prepared *via* a citrate technique from appropriate nitrates dissolved in citric acid as opposed to the ceramic method using oxides and carbonates presented here. Given that the $Sr_2Co_2O_5$ system is highly dependent on temperature (hence the existence of several different polymorphs of $Sr_2Co_2O_5$), it seems that even subtle differences in synthesis may influence the tetrahedral chain ordering adopted upon quenching to form the metastable brownmillerite-type phase. Although the *I2mb* structural model is in theory the most energetically feasible [12], it may be that synthesis conditions

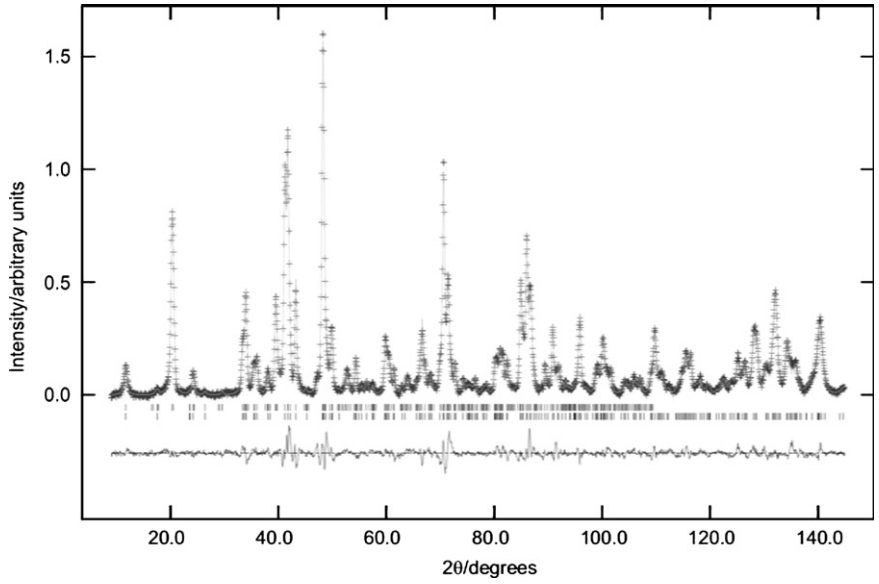

Fig. 7. Observed (+), calculated and difference NPD profiles of $Sr_2Co_2O_5$ at 4 K for refinement in the space group *Imma*; nuclear reflections are indicated by the lower vertical lines and magnetic reflections by the upper vertical lines.

prior to quenching, or perhaps very slight experimental differences in quenching rates could result in different chain ordering sequences in individual crystallites.

A recent study by Muñoz et al. [12] concluded that the correct space group for $Sr_2Co_2O_5$ was *Ima*2 (or *I*2*mb* to continue using axes consistent with the Introduction), i.e. a fully ordered brownmillerite with all tetrahedral chains having identical orientation. From the calculations presented by Muñoz et al. [12] the case for *I*2*mb* being the more stable structure appears strong. However, the assignment of a space group appropriate to a given set of diffraction data is ultimately dependent on the length scale of the experiment in comparison with the size of the ordered domains within the structure. As shown by the ED experiments, the *Pcmb* type order occurs over relatively short length scales, and XRD/NPD techniques provide information only on the average structure extending over several unit cells. Such a small domain size would result in an averaged chain orientation consistent with space group *Imma*, and refinement based on 4 K NPD data was therefore performed using *Imma*. In this space group, the octahedral ions [Co(1) and Co(3) in *Pcmb*] transform to a single site [Co(1)] and the tetrahedral Co(2) and Co(4) sites become Co(2). As for the *Pcmb* refinement, the magnetic component of the data was modelled by using a 2-phase refinement whereby one phase was purely nuclear and the other purely magnetic.

The refinement statistics for the 4 K data set ($\chi^2=5.315$, $R_{wp}=3.86\%$, $R_p=2.83\%$) were slightly inferior to those obtained using the *Pcmb* superstructure model ($\chi^2=5.080$, $R_{wp}=3.76\%$, $R_p=2.76\%$), but the difference in visual goodness of fit was negligible and the number of refined structural parameters is reduced from 33 to 15. We are therefore confident that the averaged (disordered) structure is more appropriate to represent the structure as revealed by bulk NPD data. Refinement based upon these data yielded the lattice parameters $a=5.4639(3)$ Å, $b=15.6486(8)$ Å and $c=5.5667(3)$ Å. The final observed and calculated profiles are shown in Fig. 7. Fig. 8 shows that *Imma* provides a superposition of the two chain structures present within a given tetrahedral layer corresponding to the ordered *Pcmb* space group. It therefore represents the situation for a material in which the average distance for complete L–R–L–R-chain order is insufficient for the observation of superstructure reflections. Table 1 contains the atom parameters for $Sr_2Co_2O_5$ obtained from the refinement of NPD data collected at 4 K in the space group *Imma*. The refined magnetic moment was $\mu=3.00(4)\,\mu_B$, which is in reasonable agreement with that determined by Takeda et al. ($\mu=3.3(5)\,\mu_B$ at 77 K). The moment reduction below the spin-only moment for high spin Co(III), 4 μ_B, primarily relates to covalence effects.

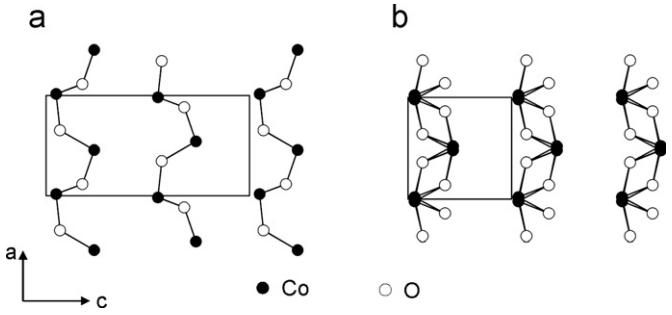

Fig. 8. The refined tetrahedral chain order and unit cells corresponding to (a) *Pcmb* and (b) *Imma* space groups. *Imma* provides a superposition of the two chain structures shown for *Pcmb*.

Table 1
Atomic parameters from the refinement of $Sr_2Co_2O_5$ in the space group *Imma* using NPD data collected at 4 K.

Atom	Site symmetry	*x*	*y*	*z*	Occupancy	$U_{iso}\times100$ (Å^2)
Sr	8*h*	0	0.6120(1)	0.5125(5)	1	0.66(6)
Co(1)	4*a*	0	0	0	1	1.93(2)
Co(2)	8*i*	0.480(6)	0.25	0.565(2)	0.5	2.1(4)
O(1)	8*g*	0.25	0.9936(2)	0.25	1	0.96(8)
O(2)	8*h*	0	0.1419(2)	0.0433(5)	1	0.86(8)
O(3)	8*i*	1.1389(9)	0.25	0.6420(9)	0.5	0.71(1)

$a=5.4639(3)$ Å, $b=15.6486(8)$ Å and $c=5.5667(3)$ Å.

Table 2 shows a selection of bond lengths obtained *via* Rietveld profile refinement in the space group *Imma* based upon NPD data collected between 4 and 300 K. It is seen that the anomalous changes in bond lengths obtained using *Pcmb* symmetry have now been eliminated from the refinements.

Bond valence sum calculations were carried out using the bond lengths derived from the refinement of NPD data in the *Imma* space group and assumed all Co to be Co^{3+} [30–32]. The bond valence sums calculated at 300 K for octahedral Co(1) and tetrahedral Co(2) are 2.47 and 2.73, respectively. These values are somewhat lower than expected and suggest that the Co sites are underbonded in this structure. However, it must be remembered that Co is in the high spin state, which will have longer bonds than low spin Co(III), and only a single BVS parameter for Co(III) is available. In addition, the brownmillerite structure for $Sr_2Co_2O_5$ is metastable at the temperatures of the current study, and this instability may relate in part to an unfavourable bonding environment, especially for the octahedral Co ion.

Table 1 shows that the U_{iso} values for the Co ions are rather high, suggesting that slightly more flexibility is required to describe the average symmetry which is consistent with the true local symmetry being *Pcmb*. However, although electron diffraction studies irrefutably showed intralayer chain ordering, the short range of the interlayer order consistent with the space group *Pcmb* results in an overall structure that is better described by the disordered space group *Imma* on the larger scale applicable to neutron (and X-ray) powder diffraction.

4. Conclusions

ED and HREM images proved the presence of L-R-L-R-intra-plane ordering of the tetrahedral chains in $Sr_2Co_2O_5$, necessitating a doubling of the *c*-parameter. However, the layers themselves were found to order according to the space group *Pcmb* over short range only. The NPD data did not show any superstructure reflections corresponding

Table 2
Selected bond lengths from NPD data collected between 4 and 300 K refined in the space group *Imma*.

Bond	Bond length (Å) at 4 K	Bond length (Å) at 100 K	Bond length (Å) at 200 K	Bond length (Å) at 300 K
Co(1)–O(1) [×4] eq	1.9527(2)	1.9526(2)	1.954(2)	1.9543(2)
Co(1)–O(2) [×2] ap	2.235(3)	2.241(3)	2.248(3)	2.249(3)
Co(2)–O(2) [×2]	1.803(5)	1.806(5)	1.808(5)	1.794(5)
Co(2)–O(3)	1.85(2), 1.89(1)	1.83(2), 1.89(1)	1.81(2), 1.91(1)	1.85(2), 1.95(1)

to the doubling of the *c*-parameter. However, Rietveld refinement based on NPD data using the space group *Pcmb* yielded an unusually short refined bond length for Co(4)–O(4) coupled with a longer Co(4)–Co(6) refined bond length, and the Co–O polyhedra from this refinement were rather dissimilar in size. Although the *Pcmb* space group permitted such elongations and contractions in bond length, there was no evidence from the NPD data that such distortions were actually present in the structure. It was postulated that the idiosyncrasies in the refinement were artefacts from the doubling of the unit cell along *c* for the refinement while the corresponding extra reflections seen on the ED patterns were not present on the NPD patterns, and the refinement in *Pcmb* did not provide a chemically satisfactory description of the overall structure of $Sr_2Co_2O_5$.

Refinement based on NPD data using space group *Imma*, provided a good fit with more feasible bond lengths. Although the L–R–L–R intralayer ordering of tetrahedral chains (and thus the assignment of the *Pcmb* space group) was incontrovertible on the basis of electron microscopy alone, on the larger scale pertinent to NPD data, the overall structure of $Sr_2Co_2O_5$ is better described using the disordered space group *Imma*.

Acknowledgments

We are grateful to Emmanuelle Suard for assistance with collection of the NPD data and Artem M. Abakumov for pointing out there could be L–R–L–R order in $Sr_2Co_2O_5$. J. H. acknowledges financial support from the European Union under the Framework 6 programme under a contract for an Integrated Infrastructure Initiative, reference 026019 ESTEEM.

References

[1] P.D. Battle, A.M. Bell, S.J. Blundell, A.I. Coldea, D.J. Gallon, F.L. Pratt, M.J. Rosseinsky, C.A. Steer, J. Solid State Chem. 167 (2002) 188.
[2] A.M. Abakumov, A.S. Kalyuzhnaya, M.G. Rozova, E.V. Antipov, J. Hadermann, G.Van Tendeloo, Solid State Sci. 7 (2005) 801.
[3] J. Hadermann, A.M. Abakumov, H. D'Hondt, A.S. Kalyuzhnaya, M.G. Rozova, M.M. Markina, M.G. Mikheev, N. Tristan, R. Klingeler, B. Büchner, E.V. Antipov, J. Mater. Chem. 17 (2007) 692.
[4] T.G. Parsons, H. D'Hondt, J. Hadermann, M.A. Hayward, Chem. Mater. 21 (2009) 5527.
[5] T. Takeda, Y. Yamaguchi, H. Watanabe, J. Phys. Soc. Jpn. 33 (1972) 970.
[6] C. Greaves, A.J. Jacobson, B.C. Tofield, B.E.F. Fender, Acta. Crystallogr. B31 (1975) 641.
[7] P.D. Battle, T.C. Gibb, P. Lightfoot, J. Solid State Chem. 76 (1988) 334.
[8] J.C. Grenier, S. Ghodbane, G. Demazeau, M. Pouchard, P. Hagenmuller, Mater. Res. Bull. 14 (1979) 831.
[9] J. Rodriguez, J.M. Gonzalez-Calbet, J.C. Grenier, J. Pannetier, M. Anne, Solid State Commun. 62 (1987) 231.
[10] W.T.A. Harrison, S.L. Hegwood, A.J. Jacobson, Chem. Commun. (1995) 1953.
[11] J.C. Grenier, L. Fournès, M. Pouchard, P. Hagenmuller, Mater. Res. Bull. 21 (1986) 441.
[12] A. Muñoz, C. de la Calle, J.A. Alonso, P.M. Botta, V. Pardo, D. Baldomir, J. Rivas, Phys. Rev. B 78 (2008) 054404.
[13] V. Pardo, P.M. Botta, D. Baldomir, J. Rivas, A. Piñeiro, C. de la Calle, J.A. Alonso, J.E. Arias, Physica B 2008 (1636) 403.
[14] C. de la Calle, A. Aguadero, J.A. Alonso, M.T. Fernandez-Diaz, Solid State Sci. 10 (2008) 1924.
[15] T. Krekels, O. Milat, G. van Tendeloo, S. Amelinckx, T.G.N. Babu, A.J. Wright, C. Greaves, J. Solid State Chem. 105 (1993) 313.
[16] S. Lambert, H. Leligny, D. Grebille, D. Pelloquin, B. Raveau, Chem. Mater. 14 (2002) 1818.
[17] A.J. Wright, H.M. Palmer, P.A. Anderson, C. Greaves, J. Mater. Chem. 11 (2001) 1324.
[18] A.M. Abakumov, M.G. Rozova, B.Ph. Pavlyuk, M.V. Lobanov, E.V. Antipov, O.I. Lebedev, G. van Tendeloo, O.L. Ignatchik, E.A. Ovtchenkov, Yu.A. Koksharov, A.N. Vasil'ev, J. Solid State Chem. 160 (2001) 353.
[19] A.M. Abakumov, A.M. Alekseeva, M.G. Rozova, E.V. Antipov, O.I. Lebedev, G. van Tendeloo, J. Solid State Chem. 174 (2003) 319.
[20] H. D'Hondt, A.M. Abakumov, J. Hadermann, A.S. Kalyuzhnaya, M.G. Rozova, E.V. Antipov, G.Van Tendeloo, Chem. Mater. 20 (2008) 7188.
[21] H. Krüger, V. Kahlenburg, Acta Crystallogr. B61 (2005) 656.
[22] H. Krüger, V. Kahlenberg, V. Petříček, F. Phillipp, W. Wertl, J. Solid State Chem. 182 (2009) 1515.
[23] A.C. Larson R.B. Von Dreele, General structure analysis system (GSAS), Los Alamos National Laboratory report LAUR 86–748, 1994.
[24] B.H. Toby, J. Appl. Cryst. 34 (2001) 210.
[25] H.M. Rietveld, Acta Crystallogr. 22 (1967) 151.
[26] H.M. Rietveld, J. Appl. Cryst. 2 (1969) 65.
[27] P. Berastegui, S.G. Eriksson S. Hull, Mater. Res. Bull. (1999) 34 (2) 303.
[28] G.J. Redhammer, G. Tippelt, G. Roth, G. Amthauer, Am. Mineral. 89 (2004) 405.
[29] F. Lindberg, G. Svenson, S. Ya., S.V. Istomin, Aleshinskaya, E.V. Antipov, J. Solid State Chem. 177 (2004) 1592.
[30] D. Altermatt, I.D. Brown, Acta Crystallogr. B41 (1985) 240.
[31] I.D. Brown, J. Solid State Chem. 82 (1989) 122.
[32] N.E. Brese, M. O'Keeffe, Acta Crystallogr. B47 (1991) 192.